analytical chemistry

pubs.acs.org/ac

Article

Electromembrane Extraction Using Sacrificial Electrodes

Frederik A. Hansen, Henrik Jensen, and Stig Pedersen-Bjergaard*

Cite This: *Anal. Chem.* 2020, 92, 5595−5603

Read Online

ACCESS | Metrics & More | Article Recommendations | Supporting Information

ABSTRACT: In this paper, we report the first example of employing a sacrificial electrode in the acceptor solution during electromembrane extraction (EME). The electrode was based on a silver wire with a layer of silver chloride electroplated onto the surface. During EME, the electrode effectively inhibited electrolysis of water in the acceptor compartment, by accepting the charge transfer across the SLM, which enabled the application of 500 μA current without suffering gas formation or pH changes from electrolysis of water. The electroplating strategy was optimized with a design-of-experiments (DOE) methodology that provided optimal conditions of electroplating. With an optimized electrode, 1 cm of the electrode in contact with the acceptor solution inhibited electrolysis of water for approximately 30 min at 500 μA current (redox capacity). Further, the redox capacity of the electrode was found to increase through multiple uses. The advantage of the electrode was demonstrated by extracting polar analytes at high-current conditions in a standard EME system comprising 2-nitrophenyl octyl ether (NPOE) as SLM and 10 mM HCl as sample/acceptor solutions. Application of high current enabled significantly higher recoveries than could otherwise be obtained at 100 μA. Sacrificial electrodes were also tested in μ-EME and were found beneficial by eliminating detrimental bubble formation. Thus, the sacrificial electrodes improved the stability of μ-EME systems. The findings of this paper are important for development of stable and robust systems for EME operated at high voltage/current and for EME performed in narrow channels/tubing where bubble formation is critical.

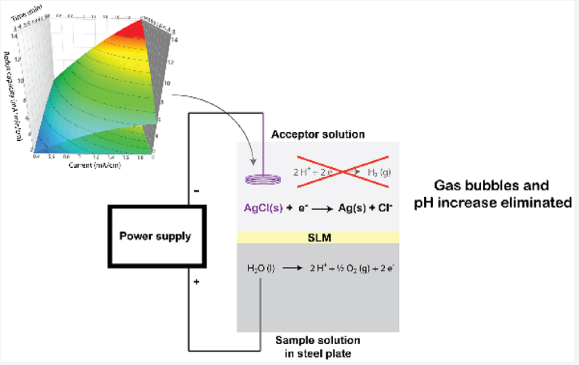

For more than two decades, miniaturization of analytical techniques for sample preparation has been an active area of research, due to several potential advantages over conventional approaches such as reduced cost and sample consumption, and environmental benefits of lower consumption of organic solvents. One such technique is electromembrane extraction (EME), which falls within the liquid-phase microextraction category. In EME, which was originally introduced in 2006,[1] two aqueous compartments holding sample and acceptor solutions, respectively, are separated by a water-immiscible organic solvent. The latter is immobilized in the pores of a polymeric membrane, to yield a supported liquid membrane (SLM) or is a free liquid membrane (FLM) squeezed between the aqueous compartments in a narrow channel. The pH-value of the aqueous solutions is adjusted to facilitate ionization of the analytes of interest. By applying an electric field across the membrane, the charged analytes are transported by electrokinetic migration into the acceptor solution. The transport of ions, both analyte and background ions, across the membrane result in generation of current, the magnitude of which is dependent on the applied voltage and the properties of the membrane. These properties may be altered in several ways by, for example, addition of ionic carriers[2−4] or employing different membrane solvents.[5−8] Such alterations may be necessary for successful extraction of polar ions, as they do not naturally partition into a hydrophobic membrane.[9,10]

However, increasing the permeability of the membrane toward polar ions will generally increase the current. The current results in electrolysis of water, as water becomes both donor and acceptor of electrons. Electrolysis results in gas formation and pH changes in the sample and acceptor compartments. Both of these effects may be devastating to a successful extraction, and consequently it is a general rule-of-thumb to keep the current below 50 to 100 μA.[11] Several reports have described how the extraction recovery typically increases with extraction time, until a certain point where it starts to decrease,[1,11−15] due to changes in the acceptor solution's pH-value. This causes loss of analyte ionization and may result in back-extraction by passive diffusion. Even minor changes in the pH of the acceptor solution may have a negative impact on the extraction efficiency. Previous reports have described the formation of a boundary layer at the membrane/

Received: February 12, 2020
Accepted: March 23, 2020
Published: March 23, 2020

acceptor interface[16−21] during EME, where pH is higher than in bulk acceptor solution. As Restan et al.[21] described, this means in practice that the acceptor solution's pH should be at least 3−4 units lower than the pK_a-value of the analyte of interest for basic analytes, in order not to affect the extraction yield negatively. pH may be stabilized by adding a high concentration of pH modifier[22] (e.g., hydrochloric or formic acid) or by using a buffer.[23] This strategy is, however, like treating the symptoms rather than the underlying cause, and even this approach may not be sufficient at high-current conditions, particularly not in μ-EME where the volumes are very small.[11] Furthermore, extreme pH is not always an option due to analyte instability or the simple fact that increased concentration of background electrolyte also increases the extraction current.

In the present contribution, we introduce for the first time the concept of sacrificial electrodes to the acceptor solution, to enable stable and robust EME under high-current EME conditions. Sacrificial metals/electrodes are frequent outside analytical chemistry to prevent oxidation of, for example, iron; however, utilization of the concept in analytical chemistry for sample preparation is very scarce. Mamat and See[24] reported the use a bubbleless electrode in EME, and although this was not a sacrificial electrode, it solved many of the problems of electrolysis. The electrode was essentially a salt-bridge that allowed the electrolytic processes to be moved away from the extraction compartments. The sacrificial electrode presented in the present work consisted of a silver wire with a sacrificial silver chloride (AgCl) layer deposited on the surface. This eliminated electrolysis of water entirely in the acceptor solution, by accepting electrons from the current flow across the SLM instead of water. The purpose of the current paper was to investigate the feasibility of sacrificial electrodes to eliminate electrolysis of water in the acceptor compartment. In addition, the fabrication of the AgCl electrode was optimized to gain the highest capacity possible for inhibition of electrolysis, and to investigate the reusability. This is the first report on EME with sacrificial electrodes, and we foresee great potential in the concept for future high-current applications and for EME in microfluidic systems.

EXPERIMENTAL SECTION

Chemicals and Reagents. Milli-Q (MQ) water was prepared by a purification system (Molsheim, France). 2-Nitrophenyl octyl ether (NPOE), bis(2-ethylhexyl) phosphate (DEHP), hydrochloric acid 37% (HCl), formic acid, ammonium acetate, trichloroacetic acid (TCA), potassium chloride, phenolphthalein, papaverine hydrochloride, mianserine hydrochloride, prochlorperazine dimaleate, haloperidol, pethdine hydrochloride, cocaine hydrochloride, methadone hydrochloride, loperamide hydrochloride, nortriptyline hydrochloride, thiamine hydrochloride, pyridoxine hydrochloride, norepinephrine bitartrate, epinephrine hydrochloride, and metformin hydrochloride were all obtained from Sigma-Aldrich (St. Louis, MO). Acetonitrile and methanol were purchased from Merck (Darmstadt, Germany). Plasma sample were obtained from Oslo University Hospital (Oslo, Norway) and stored at −32°C.

Preparation of Solutions. Stock solutions of each analyte were prepared at a concentration of 1−3 mg/mL in methanol and stored at −32°C for analytes with a positive log P value, while analytes with a negative log P value were dissolved in 30% methanol/MQ water and stored at 4 °C. Standard solutions were prepared in 10 mM hydrochloric acid by adequate dilution from stock solutions.

Preparation of AgCl Electrode. A piece of silver wire (∼8 cm, ⌀ 0.5 mm, 99.9%, K.A. Rasmussen, Hamar, Norway) was cut from a roll, and the surface was activated by a light polishing with a fine-grade sand paper. The wire was subsequently cleaned with a wipe soaked with 96% ethanol, after which approximately 5 cm of it was shaped into a coil. After the cleaning step, the electrode was only touched with gloves to avoid leaving fatty fingerprints. Five centimeters of the coiled wire was submerged into a 100 mL solution of potassium chloride (varying concentration), along with a platinum wire. The silver wire was then connected to the positive terminal (anode) of a power supply (model ES 0300e0.45, Delta Elektronika BV, Zierikzee, Netherlands), while the platinum wire (⌀ 0.5 mm, 99.9%, K.A. Rasmussen, Hamar, Norway) was connected to the negative terminal (cathode). A certain voltage/current was then applied for a given duration of time to electroplate a layer of AgCl onto the surface of the silver wire. After end plating, the AgCl electrode was flushed under Milli-Q water to remove any residual potassium chloride.

Test of AgCl Electrode's Redox Capacity. To evaluate the redox capacity of the AgCl electrode, the plated part of the electrode was submerged fully into a 100 mL solution consisting of 1 M potassium chloride for conductivity, and phenolphthalein as an indicator of rising pH. The AgCl electrode was connected to the negative terminal (cathode), while a platinum wire was used as the positive terminal (anode). A constant current of 2 mA cm^{-1} electrode was applied, and the AgCl electrode was monitored closely. As long as the electrode had capacity for inhibiting reduction of water, there was no visible change in the surroundings of the electrode. At the point where no redox capacity was left, a purple zone formed rapidly around the electrode due to increasing pH, and a few seconds after, a significant amount of gas bubbles was also observed. The time point of the onset of the purple zone's formation was recorded as the loss of redox capacity.

EME Procedure. Extractions were performed in a 96-well system, comprising a laboratory-built stainless steel plate with wells, and a commercially available 96-well MultiScreen-IP filter plate with polyvinylidene fluoride (PVDF) filter membranes with 0.45 μm pore size (Merck Millipore Ltd., Carrigtwohill, Ireland). Prior to use, 3 μL of SLM solvent (typically NPOE) was immobilized into the pores of the membrane. A 100 μL amount of sample solution was loaded into a well of the steel plate, while 100 μL of acceptor solution was loaded into the MultiScreen filter well. The filter plate and steel plate were then clamped together, and the coiled electrode was inserted into the acceptor solution though a rubber stopper. See Supporting Information 1 for pictures. A model ES 0300e0.45 (Delta Elektronika BV, Zierikzee, Netherlands) was used as power supply, by connecting the anode to the steel plate holding the sample, and the cathode to the electrode in contact with the acceptor solution. A Vibramax 100 Heidolph shaking board (Kellheim, Germany) was used to agitate the extraction system at 900 rpm. Extractions were performed for 15 min at a constant current.

μ-EME Procedure. The basic principle and instrumentation of μ-EME has previously been described in detail,[25] and we refer to this for an elaborate description. Briefly, 2 cm of PFA tubing (1/16 in. × 0.75 mm ID, Vici-Jour, Schenkon,

https://dx.doi.org/10.1021/acs.analchem.0c00626
Anal. Chem. 2020, 92, 5595−5603

Switzerland) was cut, and 0.5 μL of 1-pentanol was sandwiched between two 1.5 μL segments of aqueous solution (anolyte and catholyte) in the tubing. Electrodes (0.25 mm in diameter) were inserted from either end of the tubing into the aqueous solution and connected to a power supply (model ES 0300e0.45, Delta Elektronika BV, Zierikzee, Netherlands). The tubing was placed under a USB-microscope (QS.20200-P, Q-scope, Euromex Microscopen bv, Arnhem, The Netherlands), and photos were taken using associated software (Q-focus, v. 1.2.1.2, Euromex Microscopen bv, Arnhem, The Netherlands). The extraction current was recorded with a Fluke 287 multimeter (Everett, WA) at an acquisition rate of 8 Hz.

pH Measurements. For pH measurements of the sample and acceptor solution, the entirety of the volumes was transferred to a 0.5 mL Eppendorf tube for each, into which a pH microelectrode (Biotrode 6.0224.100, Metrohm, Switzerland) was inserted and the pH-value recorded.

Protein-Precipitation Procedure. Protein-precipitation of plasma was performed by addition of 100% w/v trichloroacetic acid (TCA) to a plasma sample at a 0.075:1 volume ratio. The mixture was then vortexed at 1800 rpm for 3 min, before being centrifuged at 10 000 rpm for 5 min. The supernatant was then collected and diluted 10-fold with Milli-Q water to produce a final pH-value of approximately 1.5.

UHPLC Conditions. The postextraction analysis of the acceptor solutions was performed by a reversed-phase (RP-UV) method for nonpolar analytes (positive log *P* value), and a hydrophilic interaction liquid chromatographic (HILIC-UV) method for polar analytes (negative log *P* value). See Table 1 for list of analytes. Both methods were run on a Dionex UltiMate 3000 RS UHPLC system comprising a pump, autosampler, column compartment, and UV-detector.

Table 1. List of Model Analytes with pK_a and log *P* values calculated by MarvinSketch 18.22 (ChemAxon, 2018)

compound	pK_a, pK_a2	log *P*
Nonpolar Analytes		
papaverine	6.03	3.08
mianserine	6.92	3.83
prochlorperazine	7.99, 2.20	4.38
haloperidol	8.05	3.66
pethidine	8.16	2.46
cocaine	8.85	2.28
methadone	9.12	5.01
loperamide	9.41	4.77
nortriptyline	10.47	4.43
Polar Analytes		
thiamine	5.54	−3.10
pyridoxine	5.58	−0.95
norepinephrine	8.85	−0.68
epinephrine	8.91	−0.43
metformin	12.33	−0.92

For the reversed-phase method, an Acquity UPLC HSS T3 column (100 mm × 2.1 mm I.D, 1.8 μm particle size) from Waters (Wexford, Ireland) maintained at 50 °C was used. The analysis was performed as a gradient elution, with mobile phase A consisting of 0.1% formic acid in 95:5 v/v MQ:ACN, and mobile phase B consisting of 0.1% formic acid in 5:95 v/v MQ:ACN. The gradient, operated at a flow of 0.5 mL/min, consisted of a linear ramp from 0 to 40% B for 0 to 15 min, where it was maintained for 2 min, before mobile phase B was increased to 80% within 0.1 min. Here it was kept for 2 min before being returned to 0% for a final 6 min re-equilibration for a total run time of 25 min. Injection volume was 5 μL, and UV-detection was performed at 210, 230, and 254 nm.

For the HILIC-UV method, an Acquity UPLC BEH amide column (150 mm × 2.1 mm I.D, 1.7 μm particle size) from Waters (Wexford, Ireland) maintained at 30 °C was used. The analysis was performed as a gradient elution, with mobile phase A consisting of 10 mM ammonium acetate in 80:20 v/v MQ:ACN, and mobile phase B consisting of 10 mM ammonium acetate in 90:10 v/v ACN:MQ. The gradient, operated at a flow of 0.5 mL/min, consisted of 2 min at 100% B, after which a linear ramp to 50% B during 5 min was made. After this, the %B was returned to 100% within 0.5 min, where it was maintained for 8.5 min for a total run time of 16 min. Injection volume was 5 μL, and UV-detection was performed at 254 and 280 nm. Prior to injection, the aqueous acceptor solution was diluted 10-fold in acetonitrile to match the initial composition of the mobile phase.

Calculations. The extraction recovery (%*R*) was calculated by the following equation for each analyte:

$$\%R = \frac{n_{a,final}}{n_{s,initial}} \times 100\% = \frac{C_{a,final}}{C_{s,initial}} \times \frac{V_a}{V_s} \times 100\%$$

where $n_{a,final}$ and $n_{s,initial}$ are the number of moles of analyte finally collected in the acceptor solution and the number of moles of analyte originally present in the sample, respectively. $C_{a,final}$ is the final concentration of analyte in the acceptor solution, $C_{s,initial}$ is the initial analyte concentration within the sample, V_a is the acceptor volume, and V_s is the sample volume.

RESULTS AND DISCUSSION

Proof-of-Concept. To test the potential for AgCl-electrodes to limit effects of electrolysis of water during EME, a model system was used comprising NPOE as SLM and 100 μL of 10 mM HCl as both sample and acceptor solution. The cathode was placed in the acceptor compartment for extraction of cationic analytes. This was chosen, as it represents one of the most commonly used systems for EME[2,12,26−30] and therefore is a good benchmark to test the concept of sacrificial electrodes against. In a normal system with platinum (Pt) electrodes, the amount of electrolysis is directly dependent on the current. Therefore, to control the amount of electrolysis, EME was performed in constant current mode, rather than the conventional approach of applying a constant voltage. In principle, the 96-well format used in the present work can generate several milliamperes of current if the maximum voltage (300 V) is applied. This is due to a relatively thin SLM (∼100 μm) and a high degree of convection. However, for proof-of-concept, 500 μA for 15 min was used, as this is the highest current previously reported in any EME system (to the best of our knowledge), though a current this high was reported to produce somewhat unstable extraction systems.[9,31] Higher currents in another system of up to 2600 μA have also been reported, but this resulted in a breakdown of the extraction system within 2 min.[32] The power supply enabled a constant current of 500 μA (±20−30 μA), with voltages typically ranging from 100 to 250 V. The effects of electrolysis of water were evaluated by the change in pH of the acceptor solution (ΔpH) during the extraction, from the measured starting pH-value of 2.04 for 10 mM HCl. Besides the AgCl

https://dx.doi.org/10.1021/acs.analchem.0c00626
Anal. Chem. 2020, 92, 5595−5603

electrode, platinum (Pt) and silver (Ag) electrodes were tested for comparison as cathodes without any redox capacity. Extractions at 100 μA (75−150 V) for 15 min were also performed to compare system performance at two different current levels. All electrodes were prepared from 5 cm of 0.5 mm thick wire shaped into a coil that allowed the wire to be inserted into the acceptor well-plate. For proof-of-concept studies, the AgCl electrode was prepared by electroplating the coiled silver wire in 1 M KCl, by connecting it to the anode of a power supply and with an inert platinum wire as the cathode. Two volts was applied until a stable current was reached after approximately 10 min.

As seen from Figure 1, pH in the acceptor solution increased 5−6 units with 500 μA for both Ag and Pt electrodes due to

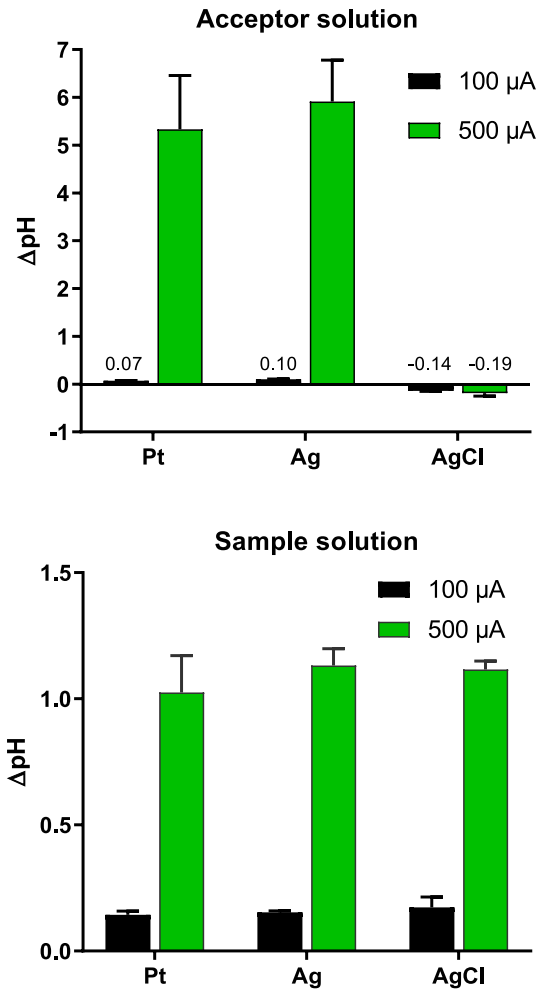

Figure 1. pH change (ΔpH) in the acceptor solution and sample solution after 15 min of extraction at 100 μA (n = 3) and 500 μA (n = 6) with Pt, Ag, and AgCl electrodes. Error bars represent standard deviation.

electrolysis, while only a minor increase was observed with 100 μA. The increase in pH was accompanied by substantial formation of gas bubbles in the acceptor and on the electrode. During the extraction, H^+ ions were reduced to $H_2(g)$ in the acceptor at a constant rate depending on the current, and pH increased with time like a titration curve. Contrary to Pt and Ag, with the AgCl electrode, pH decreased very slightly (for both 100 μA and 500 μA) and no gas bubbles were observed. This demonstrated that the AgCl electrode inhibited electrolysis of water in the acceptor compartment. We emphasize that the sacrificial electrode was only used in the acceptor compartment, and that electrolysis took place as normally in the sample. As seen from eq 1, electrolysis should result in acidification of the sample solution. Figure 1 however shows the opposite trend. The small pH decrease in acceptor and the increase in sample was explained by comigration of H^+ and OH^- ions across the SLM, from sample and acceptor, respectively. Though a constant pH is generally desirable, the minor acidification of the acceptor favored extraction of basic substances. Likewise, basic substances in the sample are not sensitive to minor pH changes in the bulk of the solution due to formation of a sample/SLM boundary rich in H^+ ions.[21]

A similar set of experiments was conducted with 10 and 50 mM phosphate buffer (Figure S3). With a Pt electrode (no redox capacity), the pH of the 50 mM acceptor increased by 0.45 ± 0.035 units from initially 1.98 after 15 min EME at 500 μA. With the Pt electrode, gas bubbles were observed. With the AgCl electrode and 50 mM phosphate, pH decreased by 0.28 ± 0.022 under similar conditions. The latter was comparable with 10 mM HCl, and this indicated that electrode redox capacity was more important than acceptor buffer capacity in this case. The pH of a sufficiently buffered solution was as such slightly more stable with a sacrificial electrode. In practice, the difference is not expected to cause any change in extraction efficiency. For some applications, good buffer capacity may thus be sufficient to stabilize the pH with a platinum electrode. However, gas formation would still pose a problem, as this previously has been reported to produce an overpressure in the compartment, leading to loss of the solution.[9] Sacrificial electrodes can eliminate this problem, in addition to stabilizing the pH-value.

Theory of Sacrificial AgCl Electrodes. In a normal EME system, electrolysis of water proceeds by the following equations, where the standard reduction potentials for the half-cell reactions[33] also are indicated for the anode (eq 1) and cathode (eq 2).

$$H_2O(l) \rightarrow 2H^+ + \frac{1}{2}O_2(g) + 2e^- \quad E^o = 1.229\ V \tag{1}$$

$$2H^+ + 2e^- \rightarrow H_2(g) \quad E^o = 0.000\ V \tag{2}$$

The reduction reaction for AgCl at the cathode can be written:

$$AgCl(s) + e^- \rightarrow Ag(s) + Cl^- \quad E^o = 0.222 \tag{3}$$

During extractions where the AgCl electrode is employed, eqs 2 and 3 are essentially competing with each other. However, due to the higher standard reduction potential of AgCl, the reduction of this will be thermodynamically favorable over that of H^+, and thus the AgCl layer on the electrode has to be consumed before electrolysis of water can take place.

The reduction of AgCl is directly proportional to the transfer of charges across the SLM, as expressed by eq 4:

$$n_{AgCl\ used} = \frac{Q}{F} = \frac{It}{F} \tag{4}$$

where $n_{AgCl\ used}$ is the moles of AgCl that have been reduced, t is time measured in seconds, Q is charges measured in Coulomb [C], F is Faraday's constant (96485 C mol^{-1}), and I is the current [A or C s^{-1}]. Equation 4 assumes a constant current throughout the extraction, but in experiments with

https://dx.doi.org/10.1021/acs.analchem.0c00626
Anal. Chem. 2020, 92, 5595−5603

varying current the total transfer of charges (Q) can be calculated by eq 5.

$$Q = \int_0^t I \, dt \tag{5}$$

From eq 3, it is apparent that chloride ions are generated in the acceptor solution during extraction. Because these ions are not expected to move into the SLM, an accumulation in the acceptor solution is expected. From eq 4, the rate of formation can be calculated to 0.62 μmol mA^{-1} min^{-1}. In our model system, comprising 500 μA for 15 min with a 100 μL acceptor solution, this corresponds to 46 mM Cl^- formed after 15 min. We do not expect this to affect the extraction, as hydrochloric acid up to 100 mM routinely is used with successful extraction. The formation of chloride may be of concern for subsequent analysis, such as capillary electrophoresis, where the conductivity of the solution may have an impact. For HPLC analysis, formation of chloride is of no concern.

In EME setups with conventional electrodes (e.g., platinum), eq 4 may also be used to estimate the theoretical pH change of the acceptor solution for a given time, current, and acceptor volume. Figure S4 shows the theoretical pH curve for the extraction conditions given in Proof-of-Concept above. This curve shows the rapid increase in pH to happen after approximately 200 s. In practice, it will however take longer time, as the observed extraction current not only is a product of the electrolytic process but also the transfer of all charged species across the SLM, including the H^+ and OH^- ions formed,[11] and other electrolytic processes.

For the sacrificial AgCl electrode, the capacity for inhibiting electrolysis of water is naturally dependent on the electrode's surface area, and hence wire length, as well as current and time. The redox capacity is therefore here characterized by the unit, mA·min·cm^{-1}.

Design and Preparation of Sacrificial AgCl electrode. To gain the highest redox capacity possible, the surface area of the electrode in contact with the acceptor solution should be large. We therefore decided to shape the electrode into a coil. For practical reasons we made the coil of 5 cm wire. Preparation of the AgCl layer was performed by electroplating the silver wire in a potassium chloride solution, with the silver wire as anode and a platinum wire as cathode. When current was passed through the system, eq 3 was essentially reversed and Ag(s) was oxidized to Ag^+, which in a chloride-rich environment formed an insoluble deposit of AgCl(s) on the electrode surface.

To assess the importance of operational parameters of the electroplating process, a design of experiments (DOE) methodology was utilized for optimization of redox capacity. The design was a central composite orthogonal (CCO) design, which included 20 experiments distributed across factorial point, star points, and 6 center points. The factors chosen for optimization were the potassium chloride (KCl) concentration of the plating solution (X1), time (X2), and current (X3), while the redox capacity of the electrode was used as the response. These factors were chosen for optimization because they were the primary parameters that affected the redox capacity. The levels of time and current were decided based on initial experiments. Here a silver wire was plated with AgCl at 2 mA cm^{-1} and at a voltage no higher than 3 V, for 15 min in 1 M KCl. The limits in terms of voltage and current were set to avoid oxygen formation during the electrode plating. Figure 2 shows a typical current profile during this process. Initially, 2

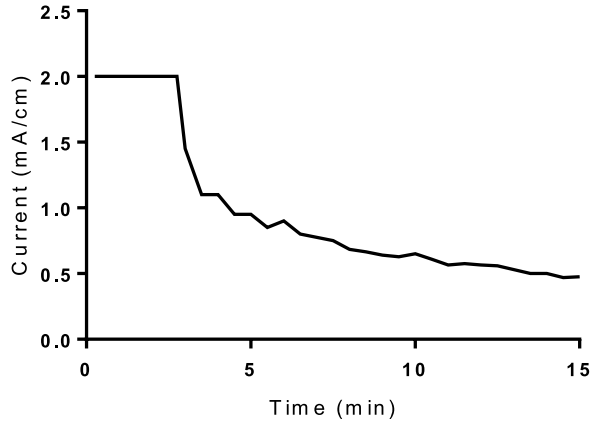

Figure 2. Typical current profile during electroplating of silver wire at 2 mA cm^{-1} or maximum 3 V for 15 min in 1 M KCl.

mA cm^{-1} could be applied with a voltage of less than 1 V. Within a few minutes, the voltage increased to the limit of 3 V, resulting in a decreasing current that ultimately formed a steady state which signified completed plating. Based on these initial experiments, the factor levels given in Table S1 were chosen and the experiments were performed. The resulting model provided a good fit of the data with a high coefficient of determination (R^2 = 0.975). All three main factors, as well as a square term of the current and interaction term of time and current (Table S2), were significant ($p < 0.05$). Further details about the quality of the model are given in Supporting Information 3.

Figure 3 visualizes the effect of the three factors by contour plots. As expected, increasing plating current and time both resulted in increased redox capacity. Interestingly, however, higher concentration of KCl in the plating solution had a small negative impact on the redox capacity, at least within the concentration range evaluated in this design. A possible explanation for this may be that during the oxidation of the silver wire, Cl^- ions can also be oxidized to Cl_2(g), which at a higher concentration creates more competition in the oxidation process. At the optimal level of the three factors, the estimated redox capacity was 14.5 mA·min·cm^{-1}.

Following completed plating of the electrode, the coated surface gained a strong purple-blackish color, as seen in Figure 4A,C. Mechanically, the coating was relatively robust and was resistant to the mechanical forces due to handling. However, when bending the wire to the preferred shape of the electrode, parts of the coating could brake off, and therefore the wire was shaped prior to electroplating. When the AgCl layer was removed completely, the electrode had a greyish appearance as seen in Figure 4B.

Regeneration of Sacrificial Electrode. The potential for regeneration of electrodes was evaluated by 10 cycles of electroplating and redox capacity testing. Testing the redox capacity implied a full removal of the AgCl coating. For further insight into the stability through multiple uses, we weighed electrodes before and after electroplating and after removal of AgCl coating. Figure 5 shows the development in redox capacity. The first test yielded 14.6 mA·min·cm^{-1}, which was almost exactly what the DOE model predicted. However, through the next few cycles, the redox capacity increased considerably, and by cycle 10 the capacity approached 30 mA·min·cm^{-1}. Thus, the redox capacity of the AgCl electrodes could easily be regenerated, and we improved capacity after

https://dx.doi.org/10.1021/acs.analchem.0c00626
Anal. Chem. 2020, 92, 5595−5603

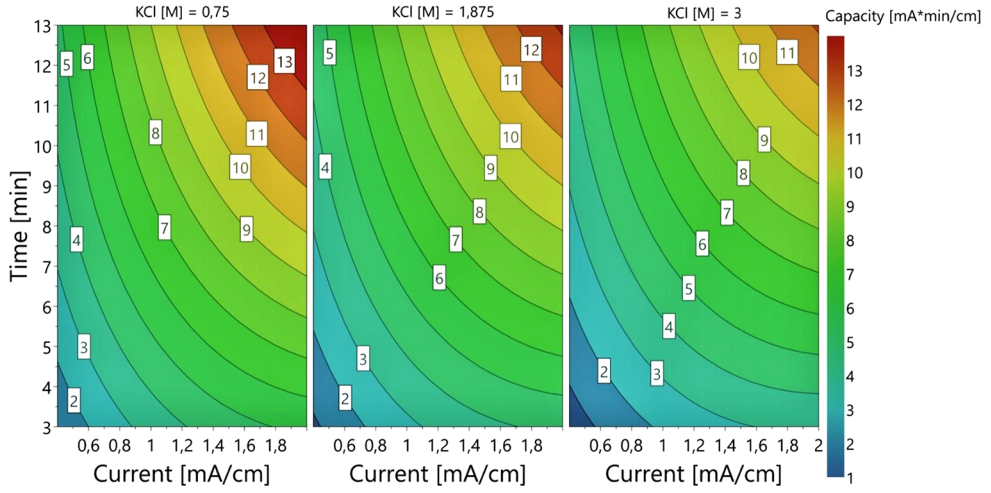

Figure 3. Contour plot of the electrode's redox capacity depending on KCl concentration, plating time, and plating current.

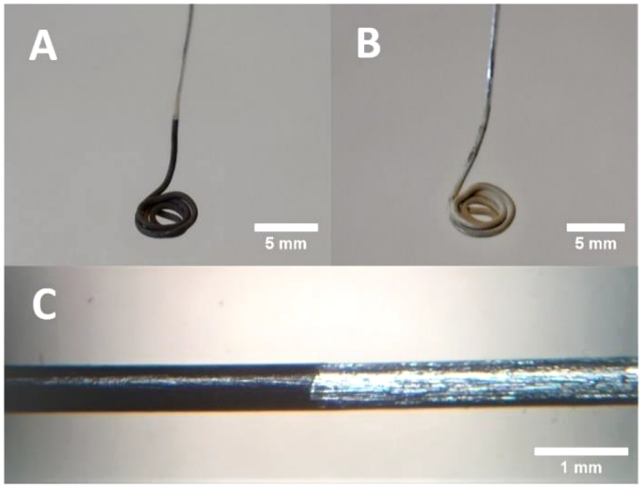

Figure 4. (A) Photo of the coiled electrode after completed electroplating of the AgCl layer. (B) Photo of the coiled electrode after completed electrochemical removal of the AgCl layer. (C) Micrograph of the coated part (left half) and the uncoated part (right half) of the electrode.

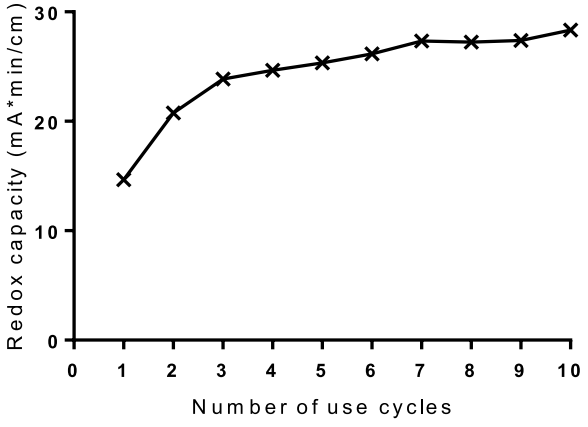

Figure 5. Development in redox capacity through multiple use cycles of an electrode. One use cycle consisted of electroplating the electrode followed by full removal of the AgCl to test the redox capacity.

multiple uses. The increase in weight during electroplating correlated (R^2 = 0.9849) with the experimental redox capacity as illustrated in Figure 6A and corresponded to the theoretical

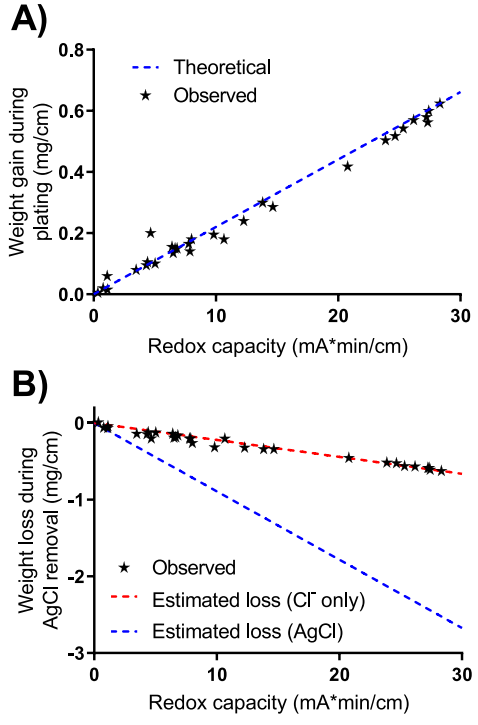

Figure 6. Weight change of electrodes with different redox capacities. (A) Increase in weight during electroplating. (B) Decrease in weight during removal of the AgCl coating. The stippled lines indicate the theoretical decrease in weight if one assumes only Cl^- is lost (red), and if also the Ag atom is lost (blue). The data points are a compilation of experiments from DOE and evaluation of reuse of electrodes.

chloride uptake as calculated from eq 4 (blue line). During removal of the AgCl coating according to eq 3, silver (Ag(s)) formed by reduction can (1) transfer into solution as colloidal silver, or (2) redeposit on the surface of the electrode. Figure 6B shows the loss of weight for the electrode during removal of the AgCl coating, with linear correlation (R^2 = 0.9779) between weight loss and redox capacity. The plot also includes

https://dx.doi.org/10.1021/acs.analchem.0c00626
Anal. Chem. 2020, 92, 5595−5603

the estimated weight loss for Cl^- only (red) and for AgCl (blue). As seen, the observed weight loss gives a strong indication that only chloride was lost during the removal of the AgCl layer, thereby leading to the conclusion that Ag(s) was redeposited on the surface of the electrode. This may explain the increase in redox capacity through multiple regenerations, as Ag redeposited with increasing porosity on the electrode surface.

Analyte Extraction at High-Current Conditions with Sacrificial Electrodes. The concept of sacrificial AgCl electrodes was then tested for real extractions under high current conditions. First, high current EME was tested for extraction of five polar bases selected as model analytes (Table 1). As discussed previously, polar analytes are difficult to extract due to their poor partitioning into the organic phase. To solve this, increased extraction voltage/current or addition of an ionic carrier such as DEHP to the SLM is required. Figure 7 shows the extraction recoveries obtained for both

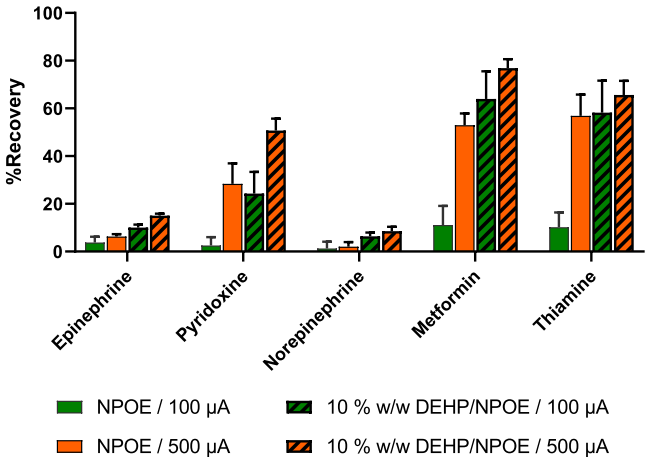

Figure 7. Extraction recoveries from 50 μg mL^{-1} of five polar bases in 10 mM HCl. The extractions were all performed with a AgCl electrode for the acceptor compartment at 100 μA or 500 μA and with either NPOE or 10% w/w DEHP/NPOE as the SLM, for 15 min. Error bars represent the standard deviation (n = 6).

strategies individually and combined. Extractions were performed at 100 or 500 μA with 10 mM HCl as sample and acceptor phase, and AgCl-coated electrodes in the acceptor phase. At 100 μA and with NPOE as SLM, all analytes were extracted with recoveries of less than 11%. Addition of DEHP to the SLM improved this considerably for pyridoxine, metformin, and thiamine, while a minor improvement was observed for epinephrine and norepinephrine. This observation is consistent with previous reports.[10] Extractions at 500 μA with NPOE, enabled by the AgCl electrode, were likewise considerably more efficient for pyridoxine, metformin, and thiamine than at 100 μA. The improvement was less for epinephrine and norepinephrine. This highlights that increasing the voltage/current is no guarantee of improving the extraction efficiency. With the DEHP/NPOE SLM, extraction efficiency also improved at high current. Despite the high current, no evidence of electrochemical degradation of analytes was found using the sacrificial electrode. Comparative extractions were performed at 500 μA with platinum electrodes. With these, pH in the acceptor increased from 2 to 8 during extraction, serious bubble formation occurred, partial or total loss of acceptor was observed, and the SLM was often damaged (Figure S8). Quantitation of the acceptor solution could therefore not be performed. The observed difference in system stability with/without sacrificial electrodes and the improved extraction efficiency of polar basic compounds at high-current conditions thus clearly demonstrated the benefits of performing EME with sacrificial electrodes.

Experiments were complemented with extraction of nine nonpolar bases (Table 1). The results are shown in Figure S9. As expected, these compounds were extracted equally efficient at 100 μA with platinum electrodes and 500 μA with sacrificial electrode. This was due to the nonpolar nature of the compounds, which enabled them to pass through the SLM under low-current conditions. We therefore emphasize that sacrificial electrodes are mainly beneficial for analytes extracted under high-current conditions. Further, to demonstrate compatibility of AgCl electrodes with biological matrixes, extractions were also performed from spiked protein-precipitated plasma samples (Figure S9). These data were in agreement with existing literature.[12,34,35] The sacrificial electrodes were thus compatible with a complex biological matrix. Between extractions, the sacrificial electrode was cleaned with ethanol to avoid carryover, similar to the typical procedure for conventional electrodes.

Application in Microelectromembrane Extraction. Kubáň and Boček performed microelectromembrane extraction (μ-EME) for the first time in 2014.[36] μ-EME differs from conventional EME by using a free liquid membrane (FLM) rather than a conventional SLM, where the organic solvent is immobilized in the pores of a supporting membrane. μ-EME is conducted in small-diameter tubing or capillary, and the volumes of solvents are just a few microliters. Due to the smaller volumes, the general tolerance to high current is therefore less in these systems. This does not only apply to pH changes but particularly also bubble formation that in the narrow tubing may disrupt the electric circuit. Application of the sacrificial electrode was therefore evaluated for μ-EME in a final set of experiments. The experimental conditions used were based on previous work.[11] As seen in Figure 8, when using a normal silver electrode without redox capacity, bubble formation (H_2) due to electrolysis at the cathode was clearly observed. After 2 min operation with tens of microampere (equal to 5.0 mC), the size of the bubble disrupted the electric circuit and extraction was no longer possible. However, with the sacrificial electrode, no bubble formation occurred. Even after testing the system equivalent to 25 mC, no bubbles formed at the cathode. This experiment clearly demonstrated the benefit of sacrificial electrodes in μ-EME. Interestingly, no bubbles were observed at the silver wire anode. Silver was oxidized under the selected μ-EME conditions and therefore essentially also functioned as a sacrificial anode. Stable pH conditions with sacrificial electrodes in μ-EME were also demonstrated, as described in Supporting Information 5.

As a miniaturized EME system, μ-EME is operated under stagnant conditions. Other miniaturized systems, such as the chip-based, are however often operated in continuous flow mode.[37−39] In this mode, pH changes of solutions are expected to be minor as fresh solution is continuously delivered. However, bubbles can still form on normal electrodes. These bubbles are expected to grow until they break off and disrupt the electric circuit. Depending on the flow rate, the bubble is expected to be flushed out of the channels, and the disruption is therefore temporary. Employing sacrificial electrodes may

https://dx.doi.org/10.1021/acs.analchem.0c00626
Anal. Chem. 2020, 92, 5595−5603

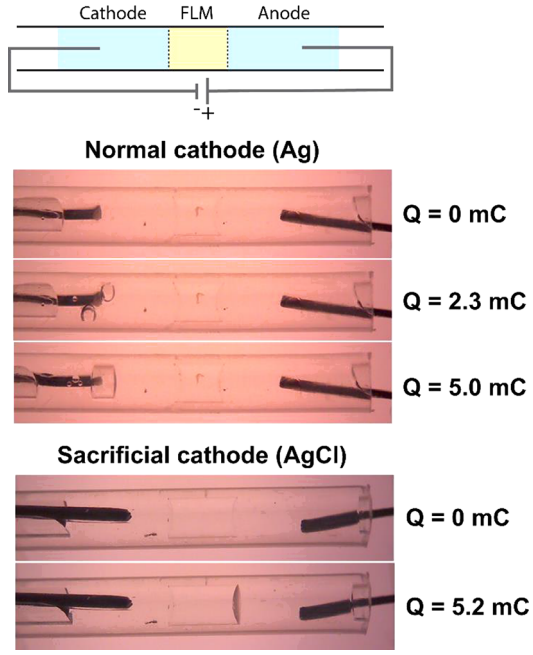

Figure 8. (Top) Illustration of μ-EME configuration. (Bottom) Photographs showing bubble formation at the cathode with a normal silver electrode and the complete lack of bubble formation with a sacrificial AgCl electrode. Experimental conditions: anolyte and catholyte were both 1.5 μL of 0.1 M formic acid, and 0.5 μL of 1-pentanol was used as FLM. Anode electrode was a 0.25 mm silver wire. Voltage: 100 V.

however still be useful to ensure the best conditions for repeatable extractions.

Comparison with Other High-Current EME Systems. Table 2 lists previous EME systems operated at high current.

Table 2. Comparison of System Stability for Different EME Systems Operating at High Current

EME format	current (μA)	inhibition of electrolysis?	system instability	ref
96-well	500	yes	stable	this work
96-well	500	no	pH increase, loss of acceptor solution	this work
96-well	500	no	overpressure and volume loss in acceptor compartment	9
96-well	300	no	stable below 300 μA	9
hollow-fiber	250	yes	stable below 250 μA	24
hollow-fiber	300	no	pH increase and bubble formation	31
96-well	400	no	overpressure and volume loss in acceptor compartment	40
flat-membrane	>100	no	decrease of recovery	7

Generally, current levels above 300 μA are reported to result in system instability when electrolysis effects have not been eliminated. Besides the present work, only the approach of Mamat and See[24] with a bubbleless electrode have eliminated electrolysis in the extraction compartments. In their approach, an in-capillary salt bridge was used to electrically connect the extraction compartment to an external compartment where the extraction voltage was applied. The electrolysis hence took place in this external compartment. Because the distance from the actual electrode to the SLM was longer, the authors applied voltages of up to 3000 V, corresponding to 250 μA, to gain efficient extraction.

CONCLUSION

The concept of sacrificial electrodes in electromembrane extraction was demonstrated for the first time. With such an electrode in the acceptor solution, electrolysis was avoided, pH was stabilized, and bubble formation was eliminated. The redox capacity of the electrode was more than adequate to stabilize the system with 500 μA current, which in a conventional system with 10 mM HCl and platinum electrodes is not feasible. This allowed several fold increase in extraction recovery of basic polar model analytes, compared to operation at lower current. The specific sacrificial electrode (AgCl) presented here only provided inhibition of electrolysis as the cathode. For acidic analytes, the electrode can thus not inhibit electrolysis in the acceptor compartment, because the anode must be placed here. The sacrificial electrode was additionally tested in a μ-EME system, providing considerably higher tolerance to high current, particularly related to bubble formation. The latter may also be useful for chip-based EME performed in narrow channels. We consider the present work to be an important step expanding the EME toolbox. Particularly, for extraction of analytes suffering from poor SLM partitioning, and for applications such as μ-EME or chip-based EME vulnerable to gas formation at the electrodes, sacrificial electrodes should be considered. Extraction of multiply charged biomolecules, such as peptides, may require a stable pH, and represents another area where sacrificial electrodes may be favorable. We expect EME to be explored for biomedical applications of increasing complexity in the future, and for such applications, the use of buffered solutions combined with sacrificial electrodes may play a key role.

ASSOCIATED CONTENT

Supporting Information

The Supporting Information is available free of charge at https://pubs.acs.org/doi/10.1021/acs.analchem.0c00626.

Graphical illustration and photos of EME setup, supplementary graphs for pH change during EME from phosphate buffer, design-of-experiments methodology and results, photos and extraction data from extraction experiments, and demonstration of inhibition of pH increases at the cathode using a sacrificial electrode in μ-EME (PDF)

AUTHOR INFORMATION

Corresponding Author

Stig Pedersen-Bjergaard − *Department of Pharmacy, University of Oslo, 0316 Oslo, Norway; Department of Pharmacy, Faculty of Health and Medical Sciences, University of Copenhagen, 2100 Copenhagen, Denmark;* orcid.org/0000-0002-1666-8043; Email: stig.pedersen-bjergaard@farmasi.uio.no

Authors

Frederik A. Hansen − *Department of Pharmacy, University of Oslo, 0316 Oslo, Norway;* orcid.org/0000-0002-1666-0447

https://dx.doi.org/10.1021/acs.analchem.0c00626
Anal. Chem. 2020, 92, 5595−5603

Henrik Jensen − *Department of Pharmacy, Faculty of Health and Medical Sciences, University of Copenhagen, 2100 Copenhagen, Denmark;* orcid.org/0000-0001-6750-2716

Complete contact information is available at: https://pubs.acs.org/10.1021/acs.analchem.0c00626

Author Contributions

The manuscript was written through contributions of all authors. All authors have given approval to the final version of the manuscript.

Notes

The authors declare no competing financial interest.

REFERENCES

(1) Pedersen-Bjergaard, S.; Rasmussen, K. E. *J. Chromatogr. A* **2006**, *1109* (2), 183−190.
(2) Gjelstad, A.; Rasmussen, K. E.; Pedersen-Bjergaard, S. *J. Chromatogr. A* **2006**, *1124* (1−2), 29−34.
(3) Balchen, M.; Jensen, H.; Reubsaet, L.; Pedersen-Bjergaard, S. *J. Sep. Sci.* **2010**, *33* (11), 1665−1672.
(4) Aladaghlo, Z.; Fakhari, A. R.; Hasheminasab, K. S. *Anal. Methods* **2017**, *9* (38), 5659−5667.
(5) Seip, K. F.; Faizi, M.; Vergel, C.; Gjelstad, A.; Pedersen-Bjergaard, S. *Anal. Bioanal. Chem.* **2014**, *406* (8), 2151−61.
(6) Huang, C.; Shen, X.; Gjelstad, A.; Pedersen-Bjergaard, S. *J. Membr. Sci.* **2018**, *548*, 176−183.
(7) Huang, C.; Gjelstad, A.; Pedersen-Bjergaard, S. *J. Membr. Sci.* **2017**, *526*, 18−24.
(8) Huang, C.; Seip, K. F.; Gjelstad, A.; Pedersen-Bjergaard, S. *Anal. Chim. Acta* **2016**, *934*, 80−87.
(9) Drouin, N.; Rudaz, S.; Schappler, J. *J. Pharm. Biomed. Anal.* **2018**, *159*, 53−59.
(10) Fernández, E.; Vårdal, L.; Vidal, L.; Canals, A.; Gjelstad, A.; Pedersen-Bjergaard, S. *Anal. Bioanal. Chem.* **2017**, *409* (17), 4215−4223.
(11) Kuban, P.; Bocek, P. *J. Chromatogr. A* **2015**, *1398*, 11−19.
(12) Kjelsen, I. J. Ø.; Gjelstad, A.; Rasmussen, K. E.; Pedersen-Bjergaard, S. *J. Chromatogr. A* **2008**, *1180* (1), 1−9.
(13) Slampova, A.; Kuban, P.; Bocek, P. *Anal. Chim. Acta* **2015**, *887*, 92−100.
(14) Lee, J.; Khalilian, F.; Bagheri, H.; Lee, H. K. *J. Chromatogr. A* **2009**, *1216* (45), 7687−93.
(15) Ramos-Payan, M.; Villar-Navarro, M.; Fernandez-Torres, R.; Callejon-Mochon, M.; Bello-Lopez, M. A. *Anal. Bioanal. Chem.* **2013**, *405* (8), 2575−2584.
(16) Rezazadeh, M.; Yamini, Y.; Seidi, S.; Esrafili, A. *J. Chromatogr. A* **2012**, *1262*, 214−218.
(17) Rezazadeh, M.; Yamini, Y.; Seidi, S.; Esrafili, A. *Anal. Chim. Acta* **2013**, *773*, 52−59.
(18) Arjomandi-Behzad, L.; Yamini, Y.; Rezazadeh, M. *Anal. Biochem.* **2013**, *438* (2), 136−143.
(19) Rezazadeh, M.; Yamini, Y.; Seidi, S.; Arjomandi-Behzad, L. *J. Chromatogr. A* **2014**, *1324*, 21−28.
(20) Mohammadi, J.; Davarani, S. S. H.; Moazami, H. R. *Anal. Chim. Acta* **2016**, *934*, 98−105.
(21) Restan, M. S.; Jensen, H.; Shen, X.; Huang, C.; Martinsen, O. G.; Kuban, P.; Gjelstad, A.; Pedersen-Bjergaard, S. *Anal. Chim. Acta* **2017**, *984*, 116−123.
(22) Slampova, A.; Kuban, P.; Bocek, P. *J. Chromatogr. A* **2016**, *1429*, 364−368.
(23) Huang, C. X.; Gjelstad, A.; Pedersen-Bjergaard, S. *J. Membr. Sci.* **2015**, *481*, 115−123.
(24) Mamat, N. A.; See, H. H. *J. Chromatogr. A* **2017**, *1504*, 9−16.
(25) Kubáň, P.; Boček, P. *J. Chromatogr. A* **2014**, *1346*, 25−33.
(26) Nojavan, S.; Fakhari, A. R. *J. Sep Sci.* **2010**, *33* (20), 3231−8.
(27) Dominguez, N. C.; Gjelstad, A.; Nadal, A. M.; Jensen, H.; Petersen, N. J.; Hansen, S. H.; Rasmussen, K. E.; Pedersen-Bjergaard, S. *J. Chromatogr. A* **2012**, *1248*, 48−54.
(28) Ahmar, H.; Fakhari, A. R.; Tabani, H.; Shahsavani, A. *Electrochim. Acta* **2013**, *96*, 117−123.
(29) Yamini, Y.; Pourali, A.; Seidi, S.; Rezazadeh, M. *Anal. Methods* **2014**, *6* (15), 5554−5565.
(30) Asl, Y. A.; Yamini, Y.; Seidi, S. *Analyst* **2016**, *141* (1), 311−318.
(31) Rahmani, T.; Rahimi, A.; Nojavan, S. *Anal. Chim. Acta* **2016**, *903*, 81−90.
(32) Rahimi, A.; Nojavan, S. *J. Sep Sci.* **2019**, *42* (2), 566−573.
(33) Bruno, T. J.; Svoronos, P. D. N. *CRC Handbook of Basic Tables for Chemical Analysis*, 2nd ed.; CRC Press: Boca Raton, 2003.
(34) Hansen, F. A.; Sticker, D.; Kutter, J. P.; Petersen, N. J.; Pedersen-Bjergaard, S. *Anal. Chem.* **2018**, *90* (15), 9322−9329.
(35) Gjelstad, A.; Rasmussen, K. E.; Pedersen-Bjergaard, S. *Anal. Bioanal. Chem.* **2009**, *393* (3), 921−928.
(36) Kuban, P.; Bocek, P. *J. Chromatogr. A* **2014**, *1337*, 32−9.
(37) Zarghampour, F.; Yamini, Y.; Baharfar, M.; Faraji, M. *Analyst* **2019**, *144* (4), 1159−1166.
(38) Roman-Hidalgo, C.; Santigosa-Murillo, E.; Ramos-Payan, M.; Petersen, N. J.; Kutter, J. P.; Pedersen-Bjergaard, S. On-chip electromembrane extraction of acidic drugs. *Electrophoresis* **2019**, *40*, 2514
(39) Ali Khan, W.; Yamini, Y.; Baharfar, M.; Balal Arain, M. *New J. Chem.* **2019**, *43* (24), 9689−9695.
(40) Drouin, N.; Kloots, T.; Schappler, J.; Rudaz, S.; Kohler, I.; Harms, A.; Lindenburg, P. W.; Hankemeier, T., Electromembrane extraction of highly polar compounds: Analysis of cardiovascular biomarkers in plasma. *Metabolites* **2020**, *10* (1).4